Science of the Total Environment

Supporting Information for

Nitrate trend reversal in Dutch dual-permeability chalk springs, evaluated by tritium - based groundwater travel time distributions.

Doi: https://doi.org/10.1016/j.scitotenv.2024.175250

Hans Peter Broers¹, Mariëlle van Vliet¹, Tano Kivits¹, Timo Brussée², Jürgen Sültenfuß³ and Dico Fraters²

¹TNO Geological Survey of the Netherlands, P.O. Box 80015, 3508 TA, Utrecht, the Netherlands

²National Institute of Public Health and the Environment, Bilthoven, The Netherlands ³Universität Bremen, Institute of Environmental Physics, Department of Oceanography, Bremen, Germany

Introduction

The supporting information includes full details about the measured nitrate and tritium concentrations and Discrete Travel Time Distribution Model (DTTDM) model outputs, including tables which summarize the results and provides additional explanatory text about the soil moisture measurements which were used as inputs to the DTTDM models elaborated in the main text. Separate sections are focused on the results of the sensitivity analysis, the evaluation of the nitrate response and the outcomes of alternative denitrification models. The tables provided detail the data used in the paper, summarizing measured tritium concentrations and DTTDM model results for the 90 springs studied.

Contents of this file

S1 Spring locations and field and laboratory methods	2
S2 Reconstructing the N leaching to groundwater at the loess plateaus	8
S3 Sensitivity analysis	10
S4 Evaluating peak concentration, time-to-peak and nitrate decline 2001 and 2018	18
S5 Evaluation of the alternative denitrification models	20
S6 Hysteresis of the spring outlet concentrations	24

S1 Spring locations and field and laboratory methods

Nitrate and sulfate

Samples were taken from the springs in Fig. S1 by employees of National Institute of Public Health and the Environment (RIVM) and the Province of Limburg. The RIVM nitrate data was analysed at the Wageningen University (WUR) with Hydrion-10 and validated at RIVM-LAC with a Dionex DX-120 system and Ion Chromatography measurements in 2001 at RIVM-LAC. In 2009 and 2018, nitrate and sulphate were analysed at the TNO laboratory using Ion Chromatography. The provincial samples of nitrate and sulphate were analysed at several laboratories, all using ion chromatography (the laboratories of the Province of Limburg and Intertek (up to 2012) and Eurofins B.V. and AL-West B.V. (from 2012 onwards). The dataset over the period 2001-2018 was complemented with historical data of the Wageningen and Utrecht University and the Water Supply of Limburg (WML). Springs at the Central Plateau were sampled by Hendrix (1985) and SO₄ and NO₃ were measured with CFA autoanalyzer. The St. Brigidabron (z.001) was measured between 1981 and 1991 by Wageningen University using Ion chromatography, in combination with ion-selective electrodes for nitrate (Van Lanen et al., 1993). The Landeus spring (z.028) was in use as public water supply and historical data of nitrate and sulfate were acquired from the WML for the period 1956-1988. Table S1 list the measured nitrate concentrations collected by Hendrix in 1984 and RIVM in 2001, 2009 and 2018 and gives information about the topographical and geological settings of the sampled springs.

Tritium

Tritium samples from the campaigns from 2008 to 2018 were measured at the Bremen Mass Spectrometric facility using the Helium-3 ingrowth method (Sültenfuß et al., 2009). Tritium samples were collected in duplicate in 1000 mL plastic bottles, following the sampling protocol of the Bremen University (Sültenfuß et al., 2009, https://www.noblegas.uni-bremen.de/eng/downloads/hints for sampling 2016.pdf). After gas extraction, the samples were stored in glass for Helium-3 ingrowth for a period of 6-8 months. This approach yields detection limits of <0.1 TU for ³H. Tritium concentrations of the 2001 sampling campaign were measured at the Centre for Isotope Research (CIO) of the University of Groningen using gas proportional counting, yielding a typical uncertainty of 1.0-2.5% over the measured tritium concentrations. The available tritium data is summarized in Table S2.

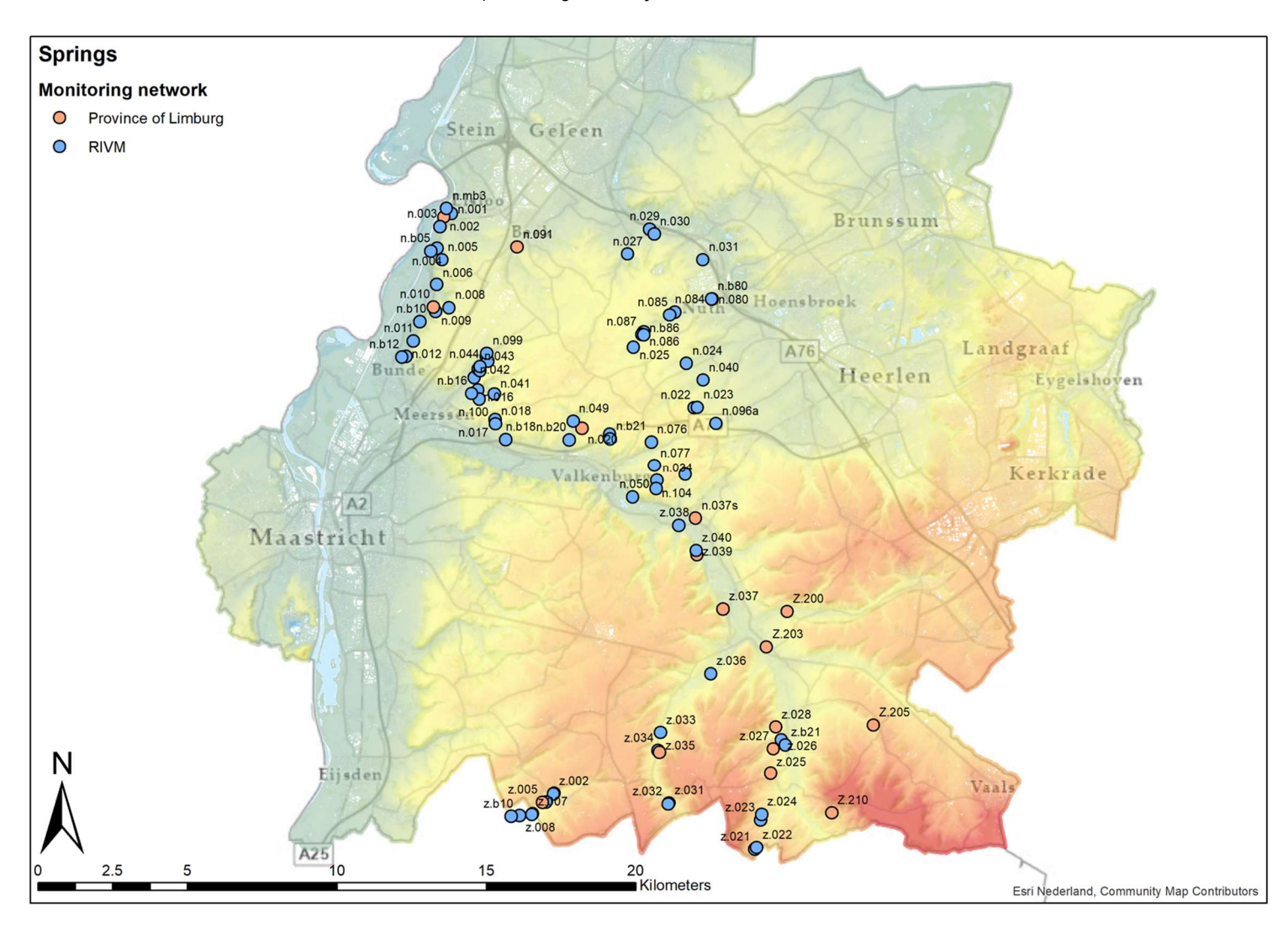


Fig. S1 Map of the locations and location codes of the sampled springs

Table S1 Measured nitrate concentrations in 1984, 2001, 2009 and 2018 for the 90 springs and broad topographical and geological setting of the springs. Figures in normal fonts indicate monitoring data from the campaigns at 8-year intervals. Italic numbers indicate averaged data from the provincial campaigns for the 1984, 2001, 2009, and 2018.

		Nitrate	(mg/l)					
Spring	1984	2001	2009	2018	Spring typology	geological formations involved in flow		
n.001	101	82		91	Hillslopes bordering W side of the Central Plateau	Neogene, Paleogene, Quaternary		
n.002	157	128	106	103	Hillslopes bordering W side of the Central Plateau	Neogene, Paleogene, Quaternary		
n.003	107	151	146	132	Hillslopes bordering W side of the Central Plateau	Neogene, Paleogene, Quaternary		
n.004	87	113	86	80	Hillslopes bordering W side of the Central Plateau	Neogene, Paleogene, Quaternary		
n.005	70	205	74	79	Hillslopes bordering W side of the Central Plateau	Neogene, Paleogene, Quaternary		
n.006	80	96	99	96	Hillslopes bordering W side of the Central Plateau	Neogene, Paleogene, Quaternary		
n.008	65	100	112	109	Hillslopes bordering W side of the Central Plateau	Neogene, Paleogene, Quaternary		
n.009	61	86	85	75	Hillslopes bordering W side of the Central Plateau	Neogene, Paleogene, Quaternary		
n.010	65	86	74	73	Hillslopes bordering W side of the Central Plateau	Neogene, Paleogene, Quaternary		
n.011	81	86	99	83	Hillslopes bordering W side of the Central Plateau	Neogene, Paleogene, Quaternary		
n.012	51	38		30	Hillslopes bordering W side of the Central Plateau	Neogene, Paleogene, Quaternary		
n.015	72	104	104	94	Hillslopes/valleys at S side of the Central Plateau	Neogene, Paleogene, Quaternary		
n.016	130	150	118	98	Hillslopes/valleys at S side of the Central Plateau	Neogene, Paleogene, Quaternary		
n.017	141	92	97	96	Hillslopes/valleys at S side of the Central Plateau	Neogene, Paleogene, Quaternary		
n.018	84	45	54	49	Hillslopes/valleys at S side of the Central Plateau	Neogene, Paleogene, Quaternary		
n.020	127	247	167	40	Hillslopes/valleys at S side of the Central Plateau	Neogene, Paleogene, Quaternary		
n.021a	107	140	42		Hillslopes/valleys at S side of the Central Plateau	Neogene, Paleogene, Quaternary		
n.022	69	84	73	65	Brook valleys of the eastern Central Plateau	Neogene, Paleogene, Quaternary		
n.023	44	74	56	57	Brook valleys of the eastern Central Plateau	Neogene, Paleogene, Quaternary		
n.024	60	55		48	Brook valleys of the eastern Central Plateau	Neogene, Paleogene, Quaternary		
n.025	37	93	104	91	Brook valleys of the eastern Central Plateau	Neogene, Paleogene, Quaternary		
n.027	70	43	39	10	Brook valleys of the eastern Central Plateau	Neogene, Paleogene, Quaternary		
n.029	37	91	87	84	Brook valleys of the eastern Central Plateau	Neogene, Paleogene, Quaternary		
n.030	227	36			Brook valleys of the eastern Central Plateau	Neogene, Paleogene, Quaternary		
n.031	35	58	61		Brook valleys of the eastern Central Plateau	Neogene, Paleogene, Quaternary		
n.034	99	106	53		Hillslopes/valleys at S side of the Central Plateau	Neogene, Paleogene, Quaternary		
n.035	71	129	121	88	Hillslopes/valleys at S side of the Central Plateau	Neogene, Paleogene, Quaternary		
n.037b	48	46	94	66	Incised regional river valleys	Neogene, Paleogene, Quaternary		
n.037s		79	47	47	Incised regional river valleys	Cretaceous Chalk & deeper formations		
n.040	42	66	56	56	Brook valleys of the eastern Central Plateau	Neogene, Paleogene, Quaternary		
n.041	59	89	47	33	Hillslopes/valleys at S side of the Central Plateau	Neogene, Paleogene, Quaternary		
n.042	92	103		62	Hillslopes/valleys at S side of the Central Plateau	Neogene, Paleogene, Quaternary		
n.043	44	125		57	Hillslopes/valleys at S side of the Central Plateau	Neogene, Paleogene, Quaternary		
n.043b	0	154		124	Hillslopes/valleys at S side of the Central Plateau	Neogene, Paleogene, Quaternary		
n.044	40	244	178	128	Hillslopes/valleys at S side of the Central Plateau	Neogene, Paleogene, Quaternary		
n.049	154	37	182	80	Hillslopes/valleys at S side of the Central Plateau	Neogene, Paleogene, Quaternary		
n.050	209	95	36	36	Incised regional river valleys	Cretaceous Chalk & deeper formations		
n.076	98	95	77	53	Hillslopes/valleys at S side of the Central Plateau	Neogene, Paleogene, Quaternary		
n.077	79	40	58	46	Hillslopes/valleys at S side of the Central Plateau	Neogene, Paleogene, Quaternary		
n.080	78	100		44	Brook valleys of the eastern Central Plateau	Neogene, Paleogene, Quaternary		
n.084	105	79	63	84	Brook valleys of the eastern Central Plateau	Neogene, Paleogene, Quaternary		
n.085	79	87	78	78	Brook valleys of the eastern Central Plateau	Neogene, Paleogene, Quaternary		
n.086	68	92		87	Brook valleys of the eastern Central Plateau	Neogene, Paleogene, Quaternary		
n.087	60	161	104		Brook valleys of the eastern Central Plateau Neogene, Paleogen			
n.091	99	167	83	110	Hillslopes bordering W side of the Central Plateau	Neogene, Paleogene, Quaternary		

	Nitrate (mg/l)					
Spring	1984	2001	2009	2018	Spring typology	geological formations involved in flow
n.096a		28	35	36	Brook valleys of the eastern Central Plateau	Neogene, Paleogene, Quaternary
n.099		101	99	91	Hillslopes/valleys at S side of the Central Plateau	Neogene, Paleogene, Quaternary
n.100		136	48	42	Hillslopes/valleys at S side of the Central Plateau	Neogene, Paleogene, Quaternary
n.104		147	65	40	Hillslopes and brook valleys of the Central Plateau	Neogene, Paleogene, Quaternary
n.b05		100	89	79	Hillslopes bordering W side of the Central Plateau	Neogene, Paleogene, Quaternary
n.b10		75	78	85	Hillslopes bordering W side of the Central Plateau	Neogene, Paleogene, Quaternary
n.b12		30	27	27	Hillslopes bordering W side of the Central Plateau	Neogene, Paleogene, Quaternary
n.b16		79	81	68	Hillslopes/valleys at S side of the Central Plateau	Neogene, Paleogene, Quaternary
n.b18		74	81	68	Hillslopes/valleys at S side of the Central Plateau	Neogene, Paleogene, Quaternary
n.b20		95	74	65	Hillslopes/valleys at S side of the Central Plateau	Neogene, Paleogene, Quaternary
n.b21		74	51	40	Hillslopes/valleys at S side of the Central Plateau	Neogene, Paleogene, Quaternary
n.b80		64	65	56	Brook valleys of the eastern Central Plateau	Neogene, Paleogene, Quaternary
n.b86		97	95	91	Brook valleys of the eastern Central Plateau	Neogene, Paleogene, Quaternary
n.mb3	99	92	91	91	Hillslopes bordering W side of the Central Plateau	Neogene, Paleogene, Quaternary
z.001	57	85	73	59	Halfway dry valleys at southern plateaus	Cretaceous Chalk & deeper formations
z.002		72		56	Halfway dry valleys at southern plateaus	Cretaceous Chalk & deeper formations
z.004		50	43	42	Halfway dry valleys at southern plateaus	Cretaceous Chalk & deeper formations
z.005		79	65	43	Halfway dry valleys at southern plateaus	Cretaceous Chalk & deeper formations
z.006		77	81	52	Halfway dry valleys at southern plateaus	Cretaceous Chalk & deeper formations
z.007		63		32	Halfway dry valleys at southern plateaus	Cretaceous Chalk & deeper formations
z.008		68	69	59	Halfway dry valleys at southern plateaus	Cretaceous Chalk & deeper formations
z.021		23	12	2	Halfway dry valleys at southern plateaus	Cretaceous Chalk & deeper formations
z.022		23		20	Halfway dry valleys at southern plateaus	Cretaceous Chalk & deeper formations
z.023		35	45	37	Halfway dry valleys at southern plateaus	Cretaceous Chalk & deeper formations
z.024		27	32	25	Halfway dry valleys at southern plateaus	Cretaceous Chalk & deeper formations
z.025		65	61	56	Halfway dry valleys at southern plateaus	Cretaceous Chalk & deeper formations
z.026		54		33	Halfway dry valleys at southern plateaus	Cretaceous Chalk & deeper formations
z.027		42	38	36	Halfway dry valleys at southern plateaus	Cretaceous Chalk & deeper formations
z.028	26	42	40	25	Halfway dry valleys at southern plateaus	Cretaceous Chalk & deeper formations
z.031		55	62	47	Halfway dry valleys at southern plateaus	Cretaceous Chalk & deeper formations
z.032		49		51	Halfway dry valleys at southern plateaus	Cretaceous Chalk & deeper formations
z.033		77	75		Incised regional river valleys	Cretaceous Chalk & deeper formations
z.034		31		31	Incised regional river valleys	Cretaceous Chalk & deeper formations
z.035		41	28	21	Incised regional river valleys	Cretaceous Chalk & deeper formations
z.036		63			Incised regional river valleys	Cretaceous Chalk & deeper formations
z.037		42	41	38	Incised regional river valleys	Cretaceous Chalk & deeper formations
z.038		56	54		Incised regional river valleys	Cretaceous Chalk & deeper formations
z.039		41	37	34	Incised regional river valleys	Cretaceous Chalk & deeper formations
z.040		33	33	25	Incised regional river valleys	Cretaceous Chalk & deeper formations
Z.200			46	35	Incised regional river valleys	Cretaceous Chalk & deeper formations
Z.203			20	20	Incised regional river valleys	Cretaceous Chalk & deeper formations
Z.205		48	44	44	Halfway dry valleys at southern plateaus	Cretaceous Chalk & deeper formations
Z.210			40	27	Halfway dry valleys at southern plateaus	Cretaceous Chalk & deeper formations
z.b10			57	44	Halfway dry valleys at southern plateaus	Cretaceous Chalk & deeper formations
z.b21		36	12	12	Halfway dry valleys at southern plateaus	Cretaceous Chalk & deeper formations
			·			,

Table S2 Tritium data collected at the 90 springs shown in Fig. S1 (in TU, Tritium Units). Nineteen springs are part of the provincial monitoring network and have a provincial code listed below; 13 of those were sampled 4 times for tritium over the period May 2017 until February 2018 for investigating the temporal (seasonal) variability which appears to be within the range of the measurement errors (denoted with \pm).

	range or tr								
Spring	Provincial	October	May	May	May	August	November	February	April
code	code	2001	2008	2009	2017	2017	2017	2018	2018
n.002	CPMA-002	13.4 ± 0.2		8.2 ± 0.4	5.0 ± 0.3	5.0 ± 0.2	4.7 ± 0.1	4.9 ± 0.3	4.5 ± 0.2
n.010	CPMA-034	13.3 ± 0.2		8.1 ± 0.5	4.7 ± 0.4	4.6 ± 0.2	4.6 ± 0.3	4.6 ± 0.2	3.6 ± 0.2
n.020	CPGE-062	11.8 ± 0.2	62102	6.3 ± 0.3	5.0 ± 0.4	4.8 ± 0.3	4.6 ± 0.2	5.4 ± 0.3	5.9 ± 0.8
n.037s	UBGE-001	10.6 ± 0.2	6.2 ± 0.2	6.2 ± 0.5	3.6 ± 0.2	3.8 ± 0.3	3.6 ± 0.4	3.5 ± 0.1	3.6 ± 0.4
n.091	CPGB-022	15.6 ± 0.2	0.5 + 0.2	6.6 ± 0.7	4.7 ± 0.3	4.3 ± 0.3	4.4 ± 0.3	4.5 ± 0.1	4.0 ± 0.1
z.001	MPNO-001	13.9 ± 0.2	8.5 ± 0.2	7.8 ± 1.0	4.6 ± 0.2	4.6 ± 0.2		4.8 ± 0.4	4.4 ± 0.3
z.005	MPNO-002	13.2 ± 0.2	0.4 + 0.2	7.7 ± 0.3	45.02	44102	44.04	42.02	4.1 ± 0.8
z.025	CRGE-032	14.9 ± 0.2	8.4 ± 0.2	8.0 ± 1.0	4.5 ± 0.3	4.4 ± 0.3	4.1 ± 0.1	4.2 ± 0.2	3.9 ± 0.6
z.027	CRGE-031	12.6 ± 0.2		7.6 ± 0.8	4.7 ± 0.3	4.7 ± 0.2	4.5 ± 0.2	4.4 ± 0.1	4.3 ± 0.2
z.028	CRGE-033	12.6 ± 0.2		6.7 ± 0.7	4.0 ± 0.3	4.1 ± 0.1	3.9 ± 0.1	4.0 ± 0.2	3.6 ± 0.4
z.031	MPGU-007	13.5 ± 0.2		8.0 ± 0.4	20102	20102	20102	20102	3.5 ± 0.2
z.035	CRGU-005	9.5 ± 0.2		6.0 ± 0.5	3.9 ± 0.3	3.9 ± 0.2	3.8 ± 0.2	3.9 ± 0.2	3.4 ± 0.1
z.037	MPGE-001	8.8 ± 0.2	66102	6.1 ± 0.3	40.00	40.00	20102	20104	3.4 ± 0.1
z.039	MPGE-006	9.5 ± 0.2	6.6 ± 0.2	6.2 ± 0.4	4.0 ± 0.3	4.0 ± 0.3	3.8 ± 0.3	3.9 ± 0.1	3.7 ± 0.2
Z.200	UBEY-025		6.5 ± 0.2			25.04	22.01	24.02	2.7 ± 0.1
Z.201	UBEY-002		60.00			3.5 ± 0.1	3.2 ± 0.1	3.4 ± 0.3	3.4 ± 0.1
Z.203	UBGE-002		6.8 ± 0.2		27.02	27.04	25.04	20102	3.4 ± 0.4
Z.210	VYGE-019A		6.2 ± 0.2		3.7 ± 0.2	3.7 ± 0.1	3.5 ± 0.1	3.8 ± 0.2	4.1 ± 0.3
Z.205	VYGE-058	12.6 . 0.2	7.3 ± 0.2		4.2 ± 0.3	4.1 ± 0.1	4.1 ± 0.2	4.0 ± 0.1	3.5 ± 0.3
n.001		13.6 ± 0.2		02.05					4.2 ± 0.4
n.003		15.6 ± 0.2		8.3 ± 0.5					4.5 ± 0.2
n.004		15.4 ± 0.2		7.9 ± 0.3					4.4 ± 0.5
n.005		11.9 ± 0.2		7.6 ± 0.4					4.2 ± 0.2
n.006		17.1 ± 0.2		8.2 ± 0.3					4.2 ± 0.5
n.008		18.0 ± 0.2		8.5 ± 0.4					4.9 ± 0.6
n.009		17.3 ± 0.2		7.6 ± 0.8					4.3 ± 0.3
n.011		21.3 ± 0.2		10.5 ± 0.3					4.5 ± 0.5
n.012		11.5 ± 0.2		00105					5.4 ± 0.4
n.015		17.5 ± 0.3		9.0 ± 0.5					4.8 ± 0.8
n.016		13.8 ± 0.2		7.0 ± 0.4					3.8 ± 0.2
n.017		20.6 ± 0.2		12.3 ± 0.7					4.9 ± 0.7
n.018		13.0 ± 0.2		11.9 ± 0.4					6.0 ± 0.5
n.021a		9.0 ± 0.2		6.5 ± 0.5					F 0 + 0 2
n.022		13.8 ± 0.2		11 ± 0.6					5.0 ± 0.3
n.023 n.024		9.7 ± 0.2 16.4 ± 0.2		7.2 ± 0.3					5.3 ± 0.8 5.4 ± 0.3
n.025		21.8 ± 0.2		6.4 ± 0.2					4.2 ± 0.2
				8.4 ± 0.2					4.2 ± 0.2 4.3 ± 0.5
n.027 n.029		19.2 ± 0.2 20.2 ± 0.2		8.4 ± 0.3 11.8 ± 0.7					4.3 ± 0.5 4.9 ± 0.4
n.030		10.0 ± 0.2		8.7 ± 0.5					4.9 ± 0.4 6.7 ± 0.4
n.030		15.0 ± 0.2		7.3 ± 0.3					0.7 ± 0.4
n.031		13.0 ± 0.2		6.8 ± 0.3					6.4 ± 1.0
n.035		14.8 ± 0.2		7.8 ± 0.5					3.7 ± 0.2
n.037b		9.6 ± 0.2		6.4 ± 0.5					
n.040		9.6 ± 0.2 12.6 ± 0.2		6.4 ± 0.5 6.0 ± 0.5					4.6 ± 0.6
n.040		8.6 ± 0.2		4.7 ± 0.5					4.1 ± 0.1
n.041		17.5 ± 0.4		4.7 = 0.3					2.1 ± 0.1 3.8 ± 0.1
n.042		17.5 ± 0.4 17.5 ± 0.2							4.1 ± 0.2
n.043b n.044		24.8 ± 0.4		7.3 ± 1.1					3.8 ± 0.6
n.044		18.6 ± 0.3		6.1 ± 0.2					3.9 ± 0.4
		12.1 ± 0.2							5.2 ± 0.2
n.050		8.8 ± 0.2		6.0 ± 0.2					3.2 ± 0.6

Supporting Information Broers et al. (2024). Nitrate Trend Reversal in Dutch chalk springs, https://doi.org/10.1016/j.scitotenv.2024.175250

Spring	Provincial	October	May	May	May	August	November	February	April
code	code	2001	2008	2009	2017	2017	2017	2018	2018
n.076		9.8 ± 0.2		6.3 ± 0.3					4.0 ± 0.7
n.077		9.6 ± 0.2		6.7 ± 0.3					4.1 ± 0.3
n.080		16.3 ± 0.2							4.5 ± 0.6
n.084		19.3 ± 0.2		12.6 ± 0.5					5.6 ± 0.5
n.085		22.2 ± 0.2		11.5 ± 0.4					5.6 ± 0.3
n.086		20.1 ± 0.2							3.9 ± 0.2
n.087		23.0 ± 0.2		10.6 ± 0.4					
n.096a		17.6 ± 0.2		8.3 ± 0.3					4.2 ± 0.2
n.099		13.9 ± 0.2		7.6 ± 0.7					4.7 ± 0.2
n.100		11.9 ± 0.2		7.1 ± 0.3					4.2 ± 1.0
n.104		9.2 ± 0.2		6.7 ± 0.4					4.0 ± 0.5
n.b05		15.6 ± 0.2		8.4 ± 0.7					4.2 ± 0.2
n.b10		23.2 ± 0.3		10.2 ± 1.1					4.1 ± 0.4
n.b12		13.7 ± 0.2		9.0 ± 0.8					4.5 ± 0.3
n.b16		12.3 ± 0.2		8.0 ± 0.6					4.9 ± 0.4
n.b18		18.5 ± 0.2		10.0 ± 0.4					4.1 ± 0.3
n.b20		12.8 ± 0.2		9.4 ± 0.4					4.6 ± 0.2
n.b21		12.7 ± 0.2		8.3 ± 0.7					4.9 ± 0.7
n.b80		16.2 ± 0.2		9.0 ± 0.6					4.5 ± 0.5
n.b86		19.0 ± 0.2		9.9 ± 0.3					4.6 ± 0.4
n.mb3		14.6 ± 0.2		8.3 ± 0.4					4.5 ± 0.5
z.002		12.7 ± 0.2							4.1 ± 0.3
z.004		11.8 ± 0.2		6.6 ± 0.5					4.2 ± 0.2
z.006		12.7 ± 0.2		7.8 ± 0.4					4.3 ± 0.3
z.007		13.0 ± 0.2							4.0± 0.8
z.008		13.7 ± 0.2		7.9 ± 0.9					4.0± 1.1
z.021		13.8 ± 0.2		5.8 ± 0.3					5.6 ± 0.2
z.022		13.0 ± 0.2							4.2 ± 0.3
z.023		11.8 ± 0.2		6.6 ± 0.3					3.5 ± 0.3
z.024		12.0 ± 0.2		7.5 ± 0.6					3.5 ± 0.4
z.026		12.2 ± 0.2		7.4 ± 0.5					4.3 ± 0.3
z.032		14.0 ± 0.2							4.4 ± 0.7
z.033		15.9 ± 0.2		8.8 ± 0.3					
z.034		10.7 ± 0.2							3.1 ± 0.2
z.038		9.7 ± 0.2		5.7 ± 0.2					
z.040		8.1 ± 0.2		5.9 ± 0.3					3.4 ± 0.3
z.b10		12.1 ± 0.2		8,0 ± 0.4					4.4 ± 0.2
z.b20		12.3 ± 0.2		7.7 ± 0.6					4.4 ± 0.3
z.b21		10.8 ± 0.2							5.1 ± 0.3

S2 Reconstructing the N leaching to groundwater at the loess plateaus

For the period between 1996 and 2021, we used data from two monitoring networks which sample and analyze soil moisture at the loess plateaus. The Soil Moisture Network Limburg (SMN) samples the layer between 1.3 and 1.4 m below surface at farmland plots under different farmland types. Five samples are taken at each plot and mixed to obtain a combined sample. Nitrate concentrations were measured after an *agitation extraction* using a L/S ratio of 20 between soil and milliQ-water. Measured nitrate concentrations are listed in Table S3 for the period 1996-2010 for arable lands and grasslands and silage maize (columns SMN). Surveys of nitrate concentrations in the first years of the exploitation of the network showed large variations in soil moisture concentration over short spatial distances but did not reveal relevant spatial regional differences between the five loess plateaus (Mak et al., 1999). The large variations over short-distance are reflected in the substantial interquartile ranges (IQR: P75-P25, see Table S3).

Since 2003, soil moisture was also measured in the framework of the Minerals Policy Monitoring Programme (LMM), which collects mixed samples at 50 selected farms in the Zuid-Limburg region, using 16 locations per farm which were spatially distributed over each farm. These samples were *centrifugated* and nitrate was analyzed from the extracted water. The samples were taken at 1.5 -3.0 m depth and annual data are available over the period 2003-2020 (see Table S3, columns LMM).

For the years 2003, 2006, 2008 and 2010, there is overlap between the SMN and LMM results and the average concentrations of those overlapping monitoring years were used, and the averages of both networks were summarized in Table S3 (column combined input SMN/LMM). In preparing the combined times series for the nitrate input to groundwater, we weighted the overall proportion of arable lands (0.43) and grassland/maize (0.57 on the loess plateaus). These weight factors were based on the 2006 data of crop types and crop spatial percentages as registered by Statistics Netherlands (CBS STATLINE, 2023). We applied the resulting time series (last column of Table S3) for the entire region and each of the analyzed springs, following the previously mentioned observation in Mak et al. (1999).

Table S3. Monitoring data of soil moisture in the provincial Soil Moisture Network Limburg (SMN) and the national Mineral Policies Monitoring Programme (LMM) over the period 1996-2021 and combined time series of nitrate inputs to the subsurface based on data of those two networks. Averages over all farmland parcels (SMN) and farms (LMM) at the Zuid-Limburg loess plateaus.

Year	Arable l	lands							Grass	lands and sile	age maiz	e					Nitrate input
	SMN				LMM					SMN							Combined SMN/LMM
		Average	P25	P75		Average	P25	P75		Average	P25	P75		Average	P25	P75	NO ₃
	N	(mg/l)	(mg/l)	(mg/l)	Ν	(mg/l)	(mg/l)	(mg/l)	Ν	(mg/l)	(mg/l)	(mg/l)	N	(mg/l)	(mg/l)	(mg/l)	(mg/l)
1996	69	75	25	123					106	115	28	176					98
1997	65	114	58	157					96	164	94	222					142
1998	67	105	36	129					105	120	50	168					113
1999	68	108	51	150					103	95	55	124					100
2000	61	76	19	114					94	82	24	112					80
2002	64	56	26	79					98	63	27	80					60
2003	71	87	46	110					113	79	34	104	7	79	72	87	78
2005	79	79	37	98					141	73	20	97					76
2006	68	92	50	119					101	72	23	102	18	91	64	115	86
2007													14	65	50	73	74
2008	63	78	44	114	7	87	65	93	107	58	31	73	13	47	38	58	65
2009					8	80	65	95					14	57	50	61	67
2010	66	61	33	88	7	71	55	89	112	69	21	72	14	44	36	53	61
2011					11	70	45	88					16	50	39	61	59
2012					12	68	43	99					15	47	35	61	56
2013					11	82	48	111					15	56	40	72	67
2014					11	59	36	80					17	52	39	55	55
2015					12	43	24	57					15	46	37	47	45
2016					12	47	29	50					18	39	28	46	42
2017					12	62	47	72					18	38	30	49	49
2018					12	84	63	107					18	56	38	60	68
2019					12	85	59	100					18	62	47	76	72
2020					12	93	70	124					18	55	35	69	71
2021					12	79	55	113					18	50	31	69	62

S3 Sensitivity analysis

We tested the robustness of the DTTDM approach using a simple sensitivity analysis where we compared the results of the base case model runs with a number of alternative setups. The aim of the sensitivity analysis was to test whether the DTTDM approach is robust for our application and whether uncertainties are sufficiently small to evaluate the past and future spring nitrate time series on the basis of their age distributions.

The base case model used the combined tritium time series in precipitation of the Koblenz and Emmerich stations and the nitrate time series which is described in section 2.3 of the main text, in combination with equal weights for nitrate and tritium in the least squares evaluation of best-fit models. The alternative model setups use the same information as the base case model, unless otherwise stated. The alternatives were:

- Alternative model runs 1 and 2 assessed the uncertainties involved in the applying either the Emmerich or the Koblenz tritium time series in precipitation,
- Alternative model runs 3 to 6 tested the effects of different weight factors (3 times and 10 times more weight for tritium and nitrate, respectively) in the least-squares evaluation of the 50 best-fit models,
- Alternative model runs 7 and 8 tested the effects of a respectively 15% increased or decreased nitrate leaching relative to the base case model nitrate input,
- Alternative model run 9 tested the effects of a high temporal sampling of nitrate, such as
 done in a number of provincial springs, versus the low temporal sampling done at most other
 springs.

The performance of the alternative models relative to the base case models are presented in Figures S2, S3 and S4, summarizing the results for the modelled fraction of young water (< 30 years old), the Mean Travel Time (MTT) and the nitrate forecast for the year 2035, respectively. Table S4 summarizes the age histogram for the base case model, together with the derived fractions of young water and MTT for each of the springs.

Fraction of young water and MTT

The fraction of young water (<30 years, Fig. S2) and the Mean Travel Time (MTT, Fig. S3) are fairly unsensitive to the use of alternative tritium input series of Emmerich and Koblenz, as indicated by the small diversion from the (blue) regression line from the 1:1 relation (grey line) between the base case and the alternative setup (Fig. S2A, S2B, S3A, S3B). Clearly, the fraction of young water for individual springs is evaluated differently, with young fraction deviations up to 0.2 and MTT deviations of 20 years for some extreme cases. Changing the weights of tritium and nitrate in the least squares evaluation (panels C-F in Fig. S2 and S3) has limited effects as well unless we increase the weight of tritium over nitrate 10 times (Fig. S2D and Fig. S3D). This more extreme case yields a meaningful perturbation of the linear regression slope relative to the 1:1 expectation. It leads to a compressive effect on the range of MTT's: short MTT tended to increase while long MTT generally decreased. From this, we conclude that solely using the tritium time series in the age modelling, while disregarding the information from the measured nitrate evolution is not a proper way forward; it shows the need to include both the tritium and nitrate time series, which is in line with earlier conclusions from Alikhani et al. (2016) for a number of nitrate-contaminated public supply wells in California. It is important to notice that giving 3 times more weight to tritium over nitrate or vice versa does have limited effects on the models, which points to a robust approach in general. Evaluating the effects of increased or decreased nitrate loading (Fig. S2 and S3, panels G and H) suggests a rather large effect on the

modelled young fraction and MTT. For example, longer MTTs are the result of increasing the nitrate load, which makes sense because the model reacts by adding more nitrate-free older water to compensate for the extra input. Because we have quite reliable data on the nitrate inputs from the soil moisture monitoring (see section S2), we think these findings should not have repercussions for the overall approach in our case. Importantly, uncertainties in the nitrate inputs do not seem to fundamentally affect the ordering of springs over the fraction of young waters or the MTT, nor impose large deviations between the fractions or MTT of the base case model or the alternative models for the large majority of the springs. Finally, we evaluated the effects of high versus low temporal resolution nitrate sampling (Fig. S2I and S3I). For this, we compared the DTTDM base model for provincial springs with a high temporal nitrate time series with a model that just uses the RIVM measured data for the years 1984, 2001, 2009 and 2018 for these springs (thinning of the time series). Notably, the RIVM data has higher spatial coverage and lower temporal resolution, whereas the opposite is true for the provincial monitoring setup; the two datasets are complementary in this respect. The results presented in Fig. S2I and S3I indicate that the fraction of young water and MTT are largely in line with the base case model (as indicated by the regression line which overlaps the 1:1 line, with a number of individual deviations in the range of 10 to 20 years).

2035 nitrate forecasts

Fig. S4A and S4B show that the nitrate 2035 forecast is fairly unsensitive to the use of alternative tritium input series of Emmerich and Koblenz, and to the weight factors for the nitrate and tritium least-squares evaluation (C-F panels in Fig. 4), although 10 times increasing the weight of nitrate over tritium yields larger deviations for individual springs (Fig. S4F). In general, however, the regression line deviates only marginally from the 1:1 relation between base case and alternatives. The single endpoint in the lower left corner represents a spring with a forestry dominated catchment, with less agricultural inputs of nitrate.

Logically, the 2035 forecasts are sensitive to the input concentrations of nitrate leaching (Fig. S4G and S4H), especially affecting springs with large fractions of young water, many more of which would still feature nitrate concentrations above the 50 mg//l threshold in 2025 in the case of increased nitrate inputs (Fig. S4G). Temporal thinning the number of nitrate measurements in the time series (Fig. S4I) only marginally affects the forecasted 2035 concentrations, which indicates that the DTTDM models are robust, even for the springs that have low frequency nitrate measurements.

Overall, we concluded that the DTDDM approach is robust for determining the young fractions and the MTT, when both tritium and nitrate time series are included and proper information about the leaching of nitrate is available from shallow monitoring. Therefore, we determined that the differences between the alternatives and the base model are sufficiently small to assess and order the springs based on their young fractions and MTT and use the results for evaluating the nitrate trend reversal and the long-term tail of the nitrate evolution, including the 2035 forecasts.

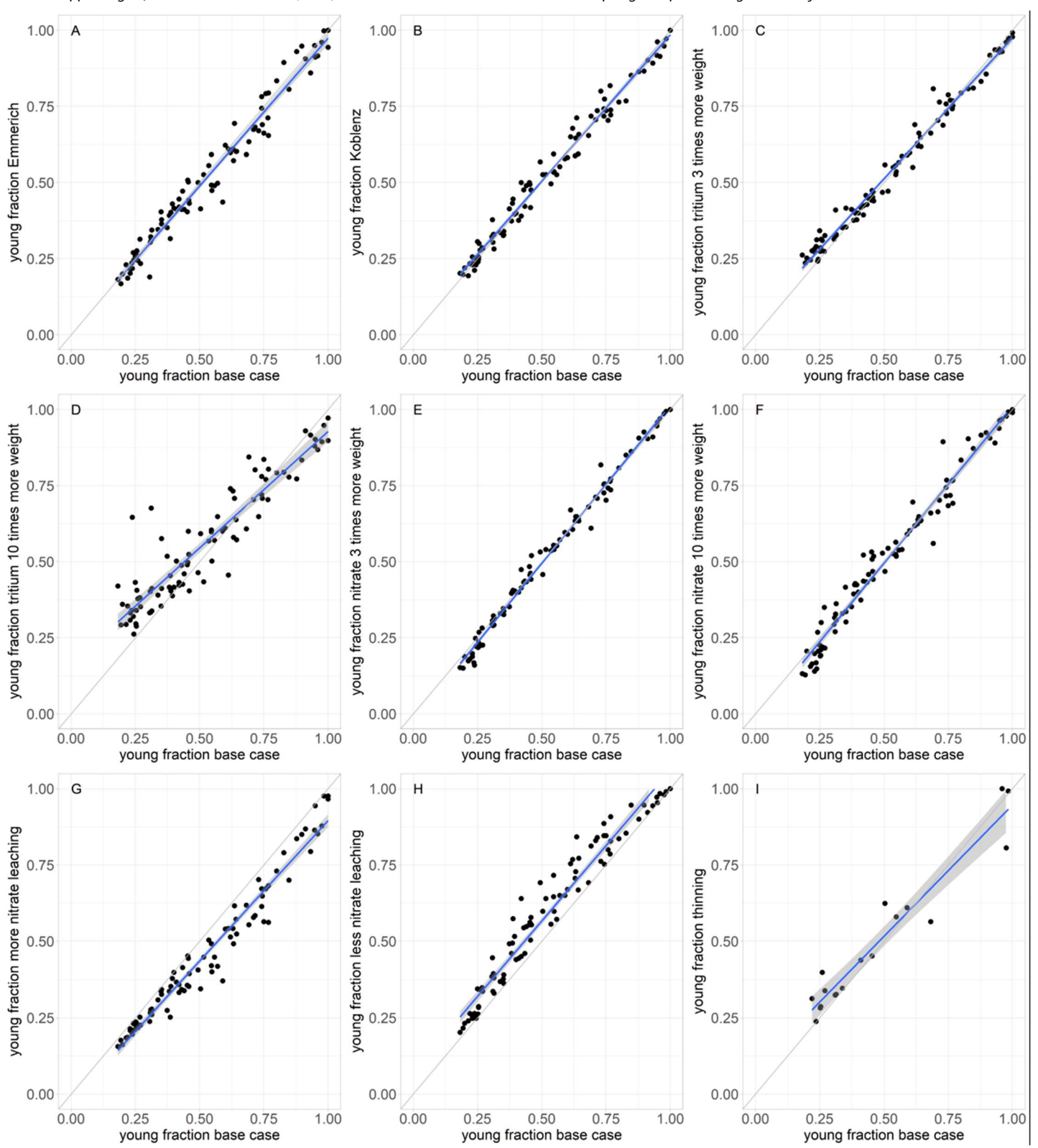


Fig. S2 Results of the sensitivity analysis: young fractions (< 30 year) for the alternative model setups (Y-axes) in comparison with the base case model (X-axis). Lines and shaded areas represent a linear regression and its uncertainty.

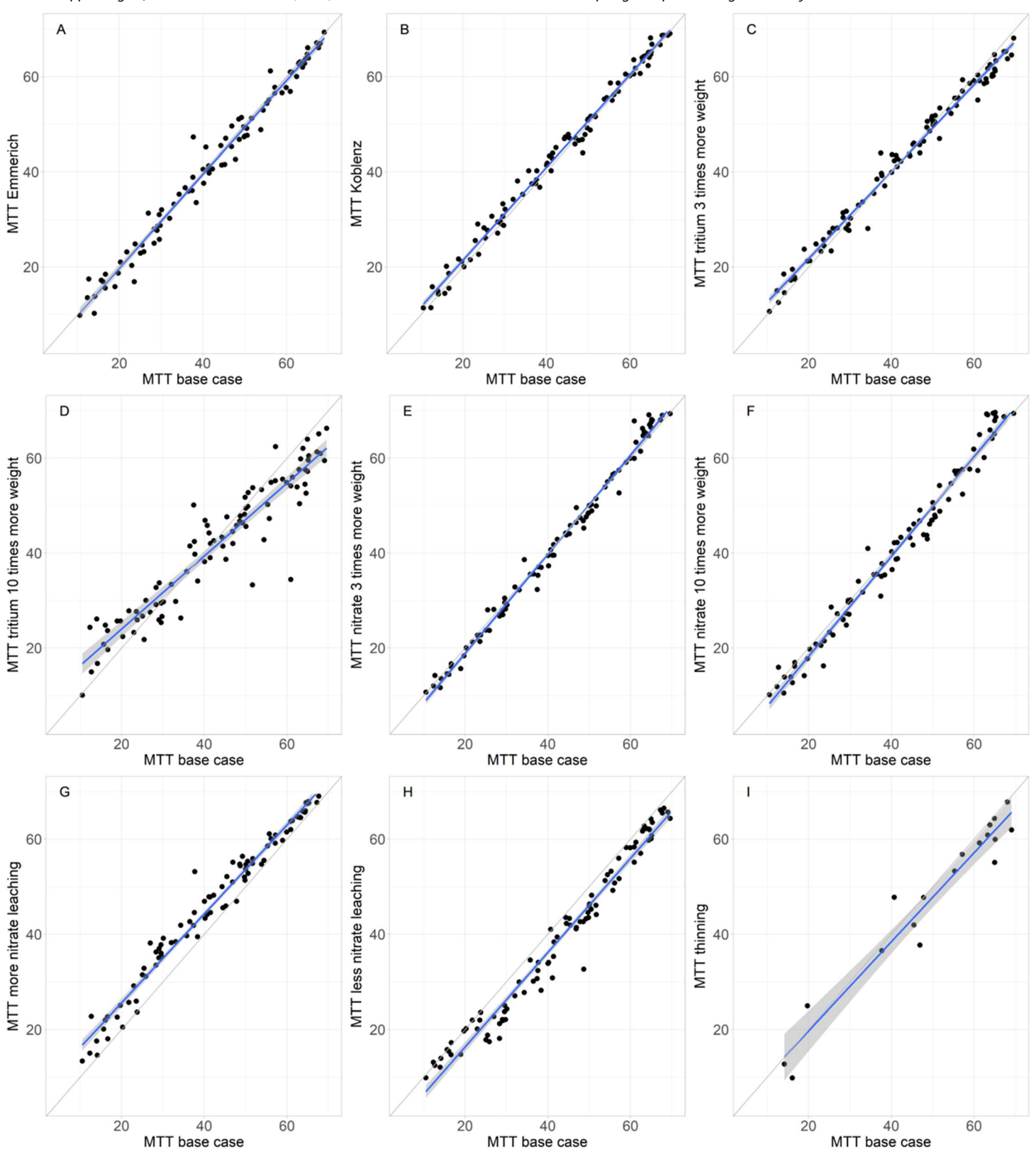


Fig. S3 Results of the sensitivity analysis: Mean Travel Time for the alternative model setups (Y-axes) in comparison with the base case model (X-). Lines and shaded areas represent a linear regression and its uncertainty.

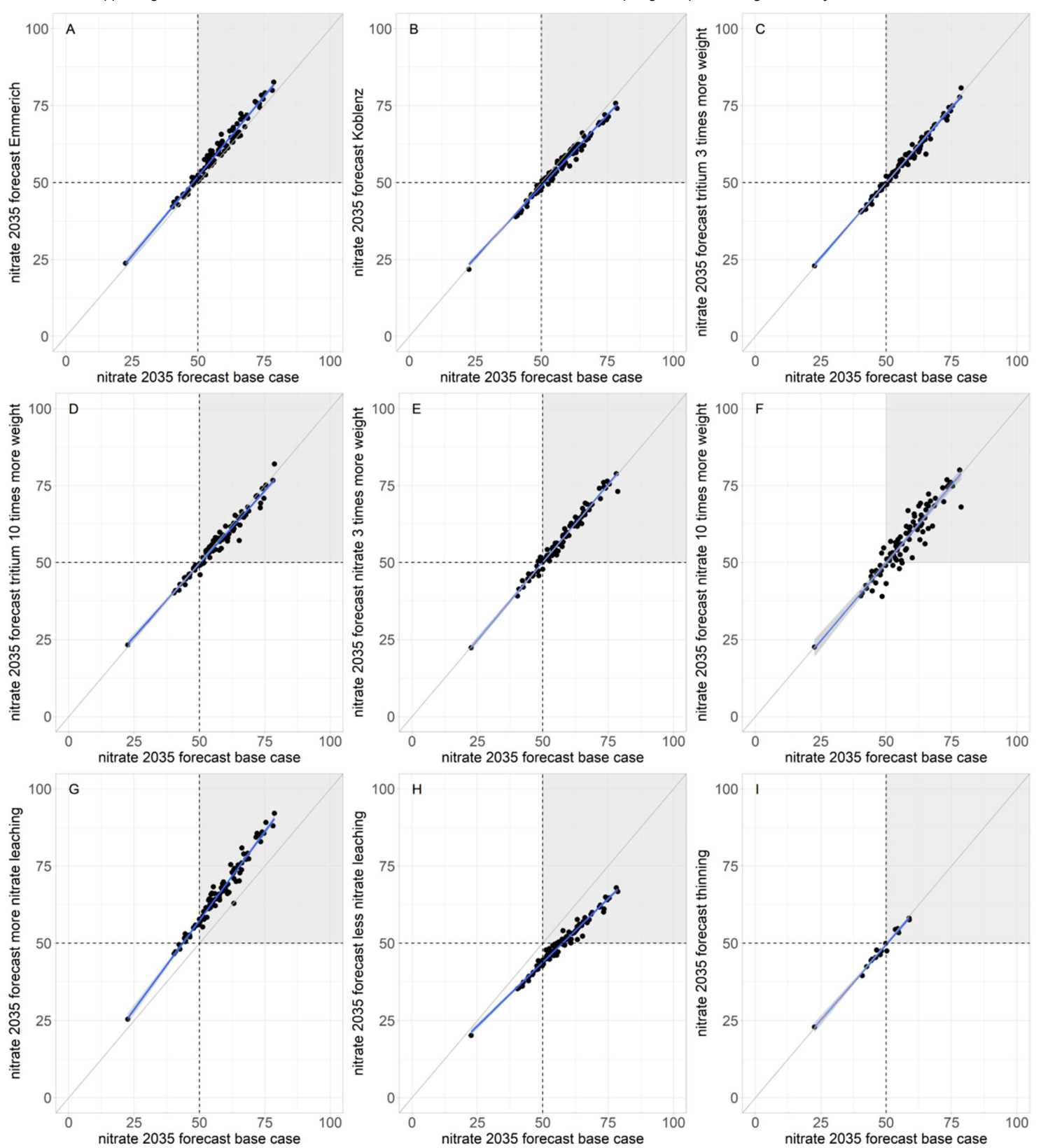


Fig. S4 Results of the sensitivity analysis: Forecasted nitrate concentration for 2035 for the alternative model setups (Y-axes) in comparison with the base case model (X-axis). The grey area denotes nitrate concentrations above the EU water quality standard of 50 mg/l. The single point in the lower left corner represents a spring with a forestry dominated catchment, with less agricultural inputs of nitrate. Lines and shaded areas represent a linear regression and its uncertainty.

Table S4. DTTDM age fractions, Mean Travel Time (MTT), combined Chi² for tritium and nitrate, and peak nitrate, lag time and concentration slope between 2001 and 2008 for the base case model. Average age fractions are given with their standard deviations of the 50 best-fit models (average ± standard deviation). Lag time is given relative to the leachate peak of 1985.

Spring	Frac	tions	MTT			Age fraction	ns (years) standa	ard deviation)			Chi ²	Peak NO3	Lag time	Slope
	< 15 yrs	< 30 yrs	(years)	0-5	5-10	10-15	15-30	30-50	50-80	> 80		(mg/l)	(years)	(mg l ⁻¹ yr ⁻¹)
n.001	0.52	0.71	28	0.27 ± 0.14	0.2 ± 0.18	0.04 ± 0.06	0.19 ± 0.08	0.1 ± 0.01	0.05 ± 0.06	0.14 ± 0.06	45.4	109.4	7	1.6
n.002	0.58	0.96	16	0.26 ± 0.15	0.23 ± 0.18	0.09 ± 0.09	0.38 ± 0.07	0.0 ± 0.0	0.0 ± 0.0	0.04 ± 0.05	37.4	133.3	13	2.6
n.003	0.41	1	17	0.1 ± 0.11	0.14 ± 0.13	0.16 ± 0.15	0.59 ± 0.11	0.0 ± 0.0	0.0 ± 0.0	0.0 ± 0.0	70.1	145.3	18	2.4
n.004	0.54	0.77	25	0.07 ± 0.08	0.39 ± 0.14	0.08 ± 0.09	0.22 ± 0.08	0.1 ± 0	0.04 ± 0.06	0.09 ± 0.06	16.7	121.8	10	2
n.005	0.84	0.95	17	0.03 ± 0.05	0.13 ± 0.13	0.68 ± 0.14	0.11 ± 0.09	0.0 ± 0.0	0.02 ± 0.04	0.04 ± 0.05	151.3	162.2	13	4.5
n.006	0.35	0.77	27	0.12 ± 0.11	0.21 ± 0.14	0.03 ± 0.04	0.42 ± 0.07	0.1 ± 0	0.05 ± 0.06	0.08 ± 0.07	33.7	112.9	19	1.2
n.008	0.21	0.75	30	0.07 ± 0.08	0.11 ± 0.11	0.04 ± 0.06	0.54 ± 0.09	0.11 ± 0.04	0.06 ± 0.06	0.08 ± 0.07	34.4	120.2	22	0.8
n.009	0.32	0.55	40	0.07 ± 0.09	0.14 ± 0.13	0.1 ± 0.11	0.23 ± 0.09	0.21 ± 0.02	0.02 ± 0.04	0.23 ± 0.05	20.7	89.6	15	0.6
n.010	0.28	0.55	46	0.09 ± 0.09	0.11 ± 0.11	0.09 ± 0.1	0.26 ± 0.09	0.11 ± 0.03	0.03 ± 0.05	0.31 ± 0.06	17	85.3	17	0.9
n.011	0.37	0.62	30	0.1 ± 0.1	0.24 ± 0.14	0.03 ± 0.05	0.25 ± 0.12	0.26 ± 0.05	0.01 ± 0.04	0.1 ± 0.06	60.6	99.5	13	0.4
n.012	0.23	0.24	60	0.12 ± 0.09	0.07 ± 0.08	0.04 ± 0.06	0.01 ± 0.03	0.2 ± 0	0.16 ± 0.12	0.4 ± 0.12	38.6	61	65	-0.3
n.015	0.31	0.72	29	0.09 ± 0.09	0.16 ± 0.11	0.06 ± 0.07	0.4 ± 0.1	0.14 ± 0.05	0.07 ± 0.07	0.08 ± 0.07	16.9	110.5	19	1
n.016	0.69	1	12	0.150 ± 0.12	0.35 ± 0.19	0.2 ± 0.14	0.31 ± 0.08	0.0 ± 0.0	0.0 ± 0.0	0.0 ± 0.0	56.8	149.2	12	3.3
n.017	0.65	0.74	16	0.38 ± 0.15	0.21 ± 0.18	0.06 ± 0.08	0.1 ± 0.09	0.26 ± 0.05	0.0 ± 0.0	0.0 ± 0.0	60.1	127.9	6	1.2
n.018	0.41	0.42	42	0.3 ± 0.11	0.08 ± 0.1	0.03 ± 0.05	0.01 ± 0.03	0.2 ± 0	0.16 ± 0.13	0.22 ± 0.12	29.9	81.8	5	0.3
n.020	0.81	0.98	14	0.05 ± 0.07	0.11 ± 0.12	0.65 ± 0.15	0.17 ± 0.12	0.0 ± 0.0	0.01 ± 0.03	0.01 ± 0.02	306.7	163.9	13	4.4
n.021a	0.8	0.8	23	0.14 ± 0.11	0.47 ± 0.18	0.19 ± 0.13	0.0 ± 0.0	0.0 ± 0.0	0.09 ± 0.08	0.11 ± 0.08	70.3	140.3	9	3.3
n.022	0.45	0.49	41	0.14 ± 0.1	0.11 ± 0.11	0.2 ± 0.12	0.05 ± 0.09	0.19 ± 0.03	0.08 ± 0.07	0.24 ± 0.07	14.2	88.3	12	1
n.023	0.32	0.4	50	0.04 ± 0.06	0.13 ± 0.1	0.15 ± 0.1	0.08 ± 0.06	0.1 ± 0	0.25 ± 0.14	0.25 ± 0.14	6.3	72.3	13	0.8
n.024	0.29	0.31	50	0.15 ± 0.11	0.09 ± 0.09	0.05 ± 0.07	0.02 ± 0.05	0.3 ± 0.02	0.08 ± 0.08	0.31 ± 0.07	29.4	74.1	42	-0.4
n.025	0.14	0.69	34	0.02 ± 0.04	0.09 ± 0.1	0.03 ± 0.06	0.55 ± 0.13	0.16 ± 0.05	0.02 ± 0.04	0.13 ± 0.08	264.1	119.2	22	0.4
n.027	0.29	0.31	52	0.11 ± 0.1	0.15 ± 0.12	0.03 ± 0.06	0.02 ± 0.04	0.3 ± 0.01	0.05 ± 0.06	0.34 ± 0.09	229.4	73.3	42	-0.4
n.029	0.22	0.46	41	0.03 ± 0.05	0.07 ± 0.09	0.12 ± 0.11	0.24 ± 0.08	0.3 ± 0	0.06 ± 0.07	0.18 ± 0.07	17.4	89.4	26	-0.2
n.030	0.89	0.91	10	0.74 ± 0.11	0.12 ± 0.13	0.03 ± 0.05	0.02 ± 0.05	0.01 ± 0.03	0.04 ± 0.06	0.04 ± 0.06	633.7	161.1	4	2.9
n.031	0.16	0.35	54	0.03 ± 0.06	0.09 ± 0.09	0.04 ± 0.06	0.19 ± 0.07	0.2 ± 0	0.11 ± 0.13	0.34 ± 0.11	49.5	68.9	29	-0.3
n.034	0.74	0.74	26	0.16 ± 0.12	0.48 ± 0.2	0.09 ± 0.08	0.01 ± 0.02	0.0 ± 0.0	0.16 ± 0.1	0.1 ± 0.08	14.7	131.5	8	2.8
n.035	0.3	0.85	29	0.05 ± 0.08	0.1 ± 0.11	0.14 ± 0.13	0.55 ± 0.13	0.02 ± 0.04	0.0 ± 0.0	0.13 ± 0.05	27.8	128.2	19	1.9
n.037b	0.17	0.39	52	0.09 ± 0.07	0.02 ± 0.04	0.06 ± 0.08	0.21 ± 0.09	0.09 ± 0.03	0.28 ± 0.15	0.24 ± 0.13	45.2	74.4	65	0.2
n.037s	0.36	0.41	55	0.08 ± 0.09	0.21 ± 0.12	0.07 ± 0.08	0.05 ± 0.06	0.1 ± 0	0.04 ± 0.05	0.45 ± 0.07	29.7	73.4	9	1
n.040	0.26	0.37	56	0.06 ± 0.07	0.12 ± 0.11	0.09 ± 0.1	0.11 ± 0.11	0.17 ± 0.05	0.04 ± 0.05	0.42 ± 0.06	25.7	65.7	13	0.4
n.041	0.33	0.46	57	0.04 ± 0.06	0.16 ± 0.14	0.12 ± 0.11	0.13 ± 0.12	0.04 ± 0.05	0.0 ± 0.0	0.5 ± 0.07	61.1	74.7	12	1.3
n.042	0.42	0.61	37	0.04 ± 0.06	0.29 ± 0.14	0.09 ± 0.11	0.19 ± 0.15	0.15 ± 0.05	0.0 ± 0.0	0.24 ± 0.05	98.6	100.2	12	1.3
n.043	0.3	0.64	36	0.02 ± 0.04	0.09 ± 0.1	0.2 ± 0.15	0.34 ± 0.18	0.17 ± 0.06	0.0 ± 0.0	0.19 ± 0.07	84.4	107.8	18	1

Spring	Frac	tions	MTT			Age fraction	ns (years) standa			Chi ²	Peak NO3	Lag time	Slope	
	< 15 yrs	< 30 yrs	(years)	0-5	5-10	10-15	15-30	30-50	50-80	> 80		(mg/l)	(years)	(mg l ⁻¹ yr ⁻¹)
n.043b	0.29	0.73	24	0.02 ± 0.04	0.07 ± 0.08	0.2 ± 0.18	0.44 ± 0.22	0.27 ± 0.08	0.0 ± 0.0	0.0 ± 0.0	92.5	127.8	23	0.6
n.044	0.28	0.95	20	0.03 ± 0.05	0.06 ± 0.08	0.2 ± 0.19	0.67 ± 0.18	0.04 ± 0.05	0.0 ± 0.0.02	0.0 ± 0.0.02	369	148.9	20	1.9
n.049	0.55	0.9	19	0.45 ± 0.11	0.07 ± 0.08	0.03 ± 0.06	0.34 ± 0.09	0.0 ± 0.0	0.03 ± 0.05	0.07 ± 0.06	450.7	122.8	6	2.2
n.050	0.87	0.88	14	0.68 ± 0.14	0.16 ± 0.14	0.04 ± 0.06	0.01 ± 0.02	0.0 ± 0.0	0.05 ± 0.06	0.07 ± 0.07	210.8	155.6	4	2.9
n.076	0.6	0.76	30	0.29 ± 0.12	0.24 ± 0.17	0.07 ± 0.08	0.16 ± 0.07	0.0 ± 0.0	0.04 ± 0.06	0.2 ± 0.06	9.6	117.4	7	2.4
n.077	0.41	0.43	51	0.25 ± 0.12	0.13 ± 0.12	0.03 ± 0.05	0.03 ± 0.05	0.1 ± 0	0.07 ± 0.08	0.39 ± 0.08	29.5	78.6	6	0.9
n.080	0.56	0.6	32	0.13 ± 0.11	0.26 ± 0.17	0.17 ± 0.13	0.04 ± 0.05	0.2 ± 0	0.03 ± 0.05	0.17 ± 0.05	36.5	108.2	9	1.4
n.084	0.53	0.55	28	0.31 ± 0.15	0.18 ± 0.16	0.04 ± 0.06	0.01 ± 0.03	0.3 ± 0	0.06 ± 0.06	0.1 ± 0.07	24.2	104.9	6	0.4
n.085	0.42	0.57	30	0.1 ± 0.11	0.28 ± 0.16	0.04 ± 0.06	0.15 ± 0.1	0.3 ± 0.02	0.02 ± 0.04	0.1 ± 0.06	43.6	99.5	10	0.4
n.086	0.26	0.52	40	0.03 ± 0.05	0.13 ± 0.12	0.1 ± 0.1	0.25 ± 0.15	0.27 ± 0.05	0.0 ± 0.0	0.21 ± 0.05	64.7	91.3	20	0.1
n.087	0.38	0.77	22	0.04 ± 0.06	0.12 ± 0.12	0.22 ± 0.19	0.38 ± 0.19	0.23 ± 0.05	0.0 ± 0.0	0.0 ± 0.0	129.9	127.4	18	1.1
n.091	0.35	0.98	20	0.05 ± 0.06	0.13 ± 0.13	0.17 ± 0.15	0.63 ± 0.11	0.0 ± 0.0	0.0 ± 0.0	0.02 ± 0.04	140.6	146.4	19	2.3
n.096a	0.15	0.18	63	0.05 ± 0.08	0.06 ± 0.09	0.03 ± 0.06	0.03 ± 0.06	0.3 ± 0.02	0.07 ± 0.07	0.45 ± 0.08	127.3	68.9	43	-1
n.099	0.26	0.64	38	0.07 ± 0.09	0.07 ± 0.08	0.12 ± 0.1	0.37 ± 0.08	0.1 ± 0	0.07 ± 0.08	0.19 ± 0.06	13.5	100.5	20	1
n.100	0.91	0.93	13	0.17 ± 0.15	0.66 ± 0.14	0.08 ± 0.09	0.02 ± 0.04	0.0 ± 0.0	0.03 ± 0.04	0.04 ± 0.05	54.4	163	8	3.7
n.104	0.83	0.83	24	0.14 ± 0.13	0.27 ± 0.18	0.41 ± 0.15	0.0 ± 0.0	0.0 ± 0.0	0.03 ± 0.06	0.14 ± 0.06	52.6	142	10	3.8
n.b05	0.34	0.63	38	0.05 ± 0.08	0.16 ± 0.15	0.13 ± 0.15	0.29 ± 0.14	0.14 ± 0.05	0.01 ± 0.04	0.22 ± 0.06	15.4	99.9	17	1.1
n.b10	0.28	0.38	42	0.07 ± 0.09	0.13 ± 0.13	0.08 ± 0.09	0.1 ± 0.08	0.4 ± 0	0.02 ± 0.04	0.2 ± 0.06	25.6	91.9	40	-0.7
n.b12	0.18	0.19	64	0.09 ± 0.1	0.07 ± 0.09	0.01 ± 0.03	0.02 ± 0.04	0.24 ± 0.05	0.08 ± 0.1	0.48 ± 0.09	60.9	61	43	-0.7
n.b16	0.27	0.54	44	0.13 ± 0.12	0.09 ± 0.09	0.06 ± 0.07	0.27 ± 0.07	0.1 ± 0	0.1 ± 0.09	0.26 ± 0.08	5.1	81.7	16	0.7
n.b18	0.25	0.43	47	0.06 ± 0.08	0.11 ± 0.12	0.08 ± 0.1	0.18 ± 0.11	0.26 ± 0.05	0.01 ± 0.03	0.29 ± 0.05	31.9	77.6	35	-0.1
n.b20	0.52	0.64	36	0.13 ± 0.12	0.26 ± 0.16	0.12 ± 0.1	0.13 ± 0.08	0.1 ± 0.01	0.02 ± 0.04	0.24 ± 0.05	9.1	105.1	9	1.8
n.b21	0.41	0.42	49	0.14 ± 0.15	0.17 ± 0.16	0.1 ± 0.1	0.01 ± 0.03	0.18 ± 0.04	0.05 ± 0.07	0.35 ± 0.09	22.2	79.1	8	0.8
n.b80	0.31	0.39	49	0.1 ± 0.12	0.14 ± 0.14	0.07 ± 0.09	0.08 ± 0.09	0.25 ± 0.05	0.04 ± 0.06	0.33 ± 0.08	21.3	70.5	10	0.1
n.b86	0.28	0.63	33	0.06 ± 0.08	0.18 ± 0.15	0.05 ± 0.07	0.35 ± 0.1	0.2 ± 0	0.05 ± 0.06	0.12 ± 0.07	23.4	102.5	20	0.5
n.mb3	0.49	0.74	26	0.27 ± 0.13	0.19 ± 0.16	0.03 ± 0.06	0.25 ± 0.06	0.1 ± 0	0.06 ± 0.07	0.1 ± 0.07	25.9	109.6	8	1.5
z.001	0.32	0.5	47	0.07 ± 0.09	0.16 ± 0.12	0.09 ± 0.1	0.18 ± 0.11	0.13 ± 0.05	0.04 ± 0.05	0.33 ± 0.05	27	81.4	13	0.8
z.002	0.33	0.44	50	0.1 ± 0.11	0.12 ± 0.13	0.11 ± 0.12	0.11 ± 0.12	0.16 ± 0.05	0.03 ± 0.05	0.37 ± 0.06	12.1	74.8	13	0.7
z.004	0.23	0.26	62	0.08 ± 0.09	0.09 ± 0.1	0.06 ± 0.07	0.03 ± 0.05	0.19 ± 0.02	0.07 ± 0.08	0.48 ± 0.07	20.7	56.5	43	-0.1
z.005	0.53	0.59	38	0.15 ± 0.16	0.32 ± 0.19	0.06 ± 0.1	0.06 ± 0.07	0.12 ± 0.04	0.03 ± 0.05	0.26 ± 0.1	26	103.4	8	1.6
z.006	0.34	0.56	44	0.12 ± 0.11	0.16 ± 0.13	0.06 ± 0.07	0.22 ± 0.08	0.1 ± 0	0.03 ± 0.05	0.31 ± 0.05	16.8	85.1	13	1
z.007	0.33	0.35	54	0.13 ± 0.13	0.12 ± 0.11	0.08 ± 0.09	0.02 ± 0.04	0.2 ± 0	0.05 ± 0.06	0.4 ± 0.08	38.7	67	8	0.3
z.008	0.32	0.39	50	0.1 ± 0.11	0.09 ± 0.1	0.13 ± 0.09	0.08 ± 0.07	0.2 ± 0	0.09 ± 0.08	0.32 ± 0.08	7.7	71.5	13	0.4
z.021	0.22	0.24	61	0.09 ± 0.11	0.1 ± 0.09	0.02 ± 0.04	0.02 ± 0.04	0.21 ± 0.02	0.13 ± 0.1	0.42 ± 0.08	197	51.5	43	-0.3
z.022	0.19	0.23	63	0.09 ± 0.12	0.08 ± 0.09	0.02 ± 0.04	0.04 ± 0.06	0.22 ± 0.04	0.07 ± 0.09	0.47 ± 0.09	71.2	50.9	43	-0.4
z.023	0.19	0.25	64	0.06 ± 0.08	0.08 ± 0.1	0.04 ± 0.07	0.06 ± 0.08	0.19 ± 0.04	0.06 ± 0.08	0.5 ± 0.08	27.3	46.9	43	-0.2

Spring	Frac	tions	MTT			Age fraction	ns (years) standa	ard deviation)			Chi ²	Peak NO3	Lag time	Slope
	< 15 yrs	< 30 yrs	(years)	0-5	5-10	10-15	15-30	30-50	50-80	> 80		(mg/l)	(years)	(mg l ⁻¹ yr ⁻¹)
z.024	0.18	0.21	65	0.08 ± 0.09	0.07 ± 0.09	0.04 ± 0.06	0.03 ± 0.06	0.21 ± 0.02	0.08 ± 0.08	0.5 ± 0.09	28.4	48.2	43	-0.3
z.025	0.32	0.45	48	0.07 ± 0.09	0.12 ± 0.13	0.13 ± 0.13	0.13 ± 0.09	0.2 ± 0.01	0.02 ± 0.04	0.33 ± 0.05	11.9	67.2	13	0.5
z.026	0.24	0.27	61	0.09 ± 0.11	0.08 ± 0.09	0.07 ± 0.09	0.02 ± 0.04	0.2 ± 0	0.07 ± 0.08	0.46 ± 0.08	33.5	57.6	43	-0.1
z.027	0.22	0.25	61	0.09 ± 0.1	0.07 ± 0.09	0.06 ± 0.08	0.04 ± 0.06	0.21 ± 0.02	0.09 ± 0.07	0.45 ± 0.05	20	50.1	43	-0.2
z.028	0.21	0.25	63	0.05 ± 0.06	0.08 ± 0.09	0.08 ± 0.09	0.05 ± 0.06	0.2 ± 0	0.06 ± 0.07	0.48 ± 0.07	37.2	48.3	43	-0.1
z.031	0.26	0.34	57	0.07 ± 0.09	0.1 ± 0.11	0.09 ± 0.09	0.08 ± 0.08	0.2 ± 0	0.02 ± 0.04	0.44 ± 0.05	25.3	62.1	13	0.2
z.032	0.24	0.31	56	0.13 ± 0.14	0.09 ± 0.1	0.02 ± 0.04	0.06 ± 0.08	0.22 ± 0.04	0.07 ± 0.09	0.4 ± 0.09	17.3	63.6	42	-0.2
z.033	0.25	0.46	45	0.05 ± 0.07	0.16 ± 0.13	0.04 ± 0.06	0.21 ± 0.08	0.2 ± 0	0.1 ± 0.11	0.24 ± 0.11	18.3	77.9	19	0.1
z.034	0.16	0.23	67	0.07 ± 0.08	0.06 ± 0.09	0.03 ± 0.06	0.07 ± 0.09	0.17 ± 0.05	0.06 ± 0.07	0.54 ± 0.07	29.5	44.1	43	-0.2
z.035	0.2	0.27	65	0.1 ± 0.1	0.07 ± 0.09	0.04 ± 0.06	0.07 ± 0.07	0.13 ± 0.05	0.08 ± 0.08	0.52 ± 0.06	29.8	43.5	65	0.1
z.036	0.25	0.31	50	0.05 ± 0.06	0.1 ± 0.1	0.1 ± 0.08	0.06 ± 0.11	0.29 ± 0.03	0.16 ± 0.14	0.25 ± 0.13	12.8	77.4	43	-0.4
z.037	0.26	0.31	64	0.11 ± 0.11	0.1 ± 0.11	0.05 ± 0.07	0.05 ± 0.07	0.1 ± 0.01	0.05 ± 0.06	0.53 ± 0.05	16.5	54.9	8	0.5
z.038	0.22	0.35	59	0.05 ± 0.07	0.13 ± 0.13	0.04 ± 0.06	0.13 ± 0.09	0.1 ± 0	0.13 ± 0.13	0.42 ± 0.11	12.1	58.9	13	0.4
z.039	0.16	0.22	69	0.08 ± 0.09	0.06 ± 0.08	0.02 ± 0.04	0.06 ± 0.07	0.13 ± 0.05	0.1 ± 0.08	0.55 ± 0.08	34.6	52.7	65	-0.1
z.040	0.21	0.25	68	0.09 ± 0.11	0.09 ± 0.09	0.04 ± 0.06	0.04 ± 0.06	0.1 ± 0.02	0.08 ± 0.08	0.56 ± 0.08	27.3	50.6	65	0.2
Z.200	0.26	0.31	65	0.06 ± 0.08	0.1 ± 0.11	0.1 ± 0.11	0.05 ± 0.07	0.11 ± 0.02	0.02 ± 0.04	0.56 ± 0.06	30.3	56.5	12	0.6
Z.203	0.23	0.24	68	0.11 ± 0.1	0.08 ± 0.1	0.04 ± 0.07	0.0 ± 0.0.01	0.12 ± 0.04	0.08 ± 0.09	0.57 ± 0.09	44.4	50	65	0.2
Z.205	0.2	0.26	65	0.09 ± 0.11	0.05 ± 0.06	0.06 ± 0.08	0.06 ± 0.07	0.13 ± 0.05	0.11 ± 0.07	0.5 ± 0.05	24.2	54.1	65	0
Z.210	0.47	0.68	41	0.08 ± 0.09	0.14 ± 0.13	0.24 ± 0.2	0.21 ± 0.12	0.0 ± 0.0.01	0.0 ± 0.0.01	0.31 ± 0.04	5.7	52.9	13	1.2
z.b10	0.41	0.45	49	0.13 ± 0.13	0.2 ± 0.18	0.08 ± 0.1	0.04 ± 0.05	0.14 ± 0.05	0.04 ± 0.06	0.36 ± 0.08	14	81.5	8	1
z.b21	0.19	0.2	65	0.1 ± 0.12	0.06 ± 0.08	0.04 ± 0.06	0.01 ± 0.03	0.19 ± 0.03	0.15 ± 0.12	0.46 ± 0.11	68.7	50.3	65	-0.3

S4 Evaluating peak concentration, time-to-peak and nitrate decline between 2001 and 2018

We evaluated the determining factors for the nitrate response following the reduction of N leaching that started in 1985 using the results of the base model of the 90 springs (Fig. S5). The figure shows that both the age fraction < 30 years and the MTT have large explanatory power for the peak of the nitrate concentration (Fig. S2A). The same holds for the explanation of the steepness of the decline of nitrate concentrations between 2001 and 2018 (second row), which is also illustrated in Fig. 4 and 5 of the main text. However, for the lag time between the peak on nitrate leaching in 1985 and the peak of nitrate concentrations in the spring, the explanatory power of the age fraction < 15 years is larger, indicating that springs with more than 50% water aged less than 15 years tend to have rather short lag time (~7-12 years), whereas small fractions of this age range concur with increased lag time. The lack of water aged less than 15 years points to storage in the unsaturated zone, which means that this young water is not yet contributing to saturated flow towards the springs. For the age fraction < 30 years, the pattern is somewhat similar but less distinctive (Fig. S5). Thus, we interpret the importance of the very young water fraction (< 15 years) to be an effect of unsaturated zone delay. Infiltrating water in areas with deep unsaturated zones will only start contributing to saturated zone flow towards the spring once water has drained from the unsaturated zone. As many of the springs at the northerly plateaus drain the more elevated parts of the aquifer system and vertical flow is limited by the presence of aquitards, their unsaturated zones are shallower, and a larger fraction of water aged less than 15 years will reach the springs. Contrary, for the springs draining the chalk aquifer, only a limited fraction of infiltrating water reaches the saturated zone in the first 15 year which enlarges the lag time.

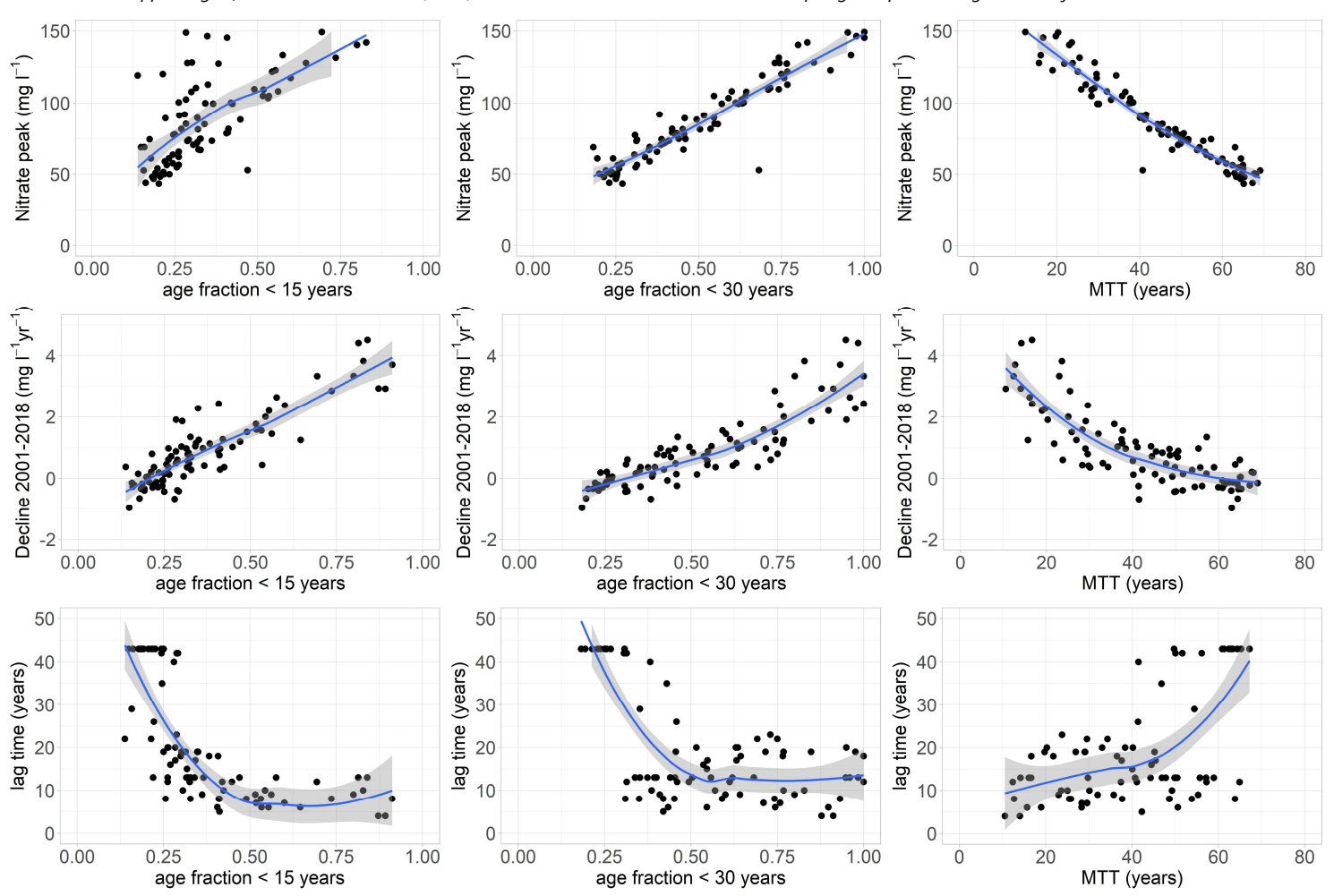


Fig. S5. Evaluating peak concentration, time-to-peak and nitrate decline between 2001 and 2018 (rows) versus the age fraction < 15 year and age fraction < 30 years and Mean Travel Time (columns) for the base case model. Lines and shaded areas represent the LOWESS smooth and its uncertainty, summarizing the local median of the data scatter (Cleveland & Devlin, 1988).

S5 Evaluation of the alternative denitrification models

The base case model and the alternative models presented in the sensitivity analysis (Section S3) all rely on the assumption of conservative transport, which is the simplest model setup which satisfies the reconstruction and forecasting of most of the springs, except for springs that have a presumed contribution from the Formation of Vaals where denitrification might play a role (see section 3.3 of the main text). Indications for denitrification processes influencing the nitrate concentrations at those wells are twofold:

- The conservative base case model and its alternatives are not able to mimic the measured decrease of nitrate concentrations in springs with an MTT of 45-60 and > 60 years and instead predict stabilizing or even slowly increasing concentrations (see Fig. 5 in main text, lower left panel).
- Sulfate concentrations in those southern springs generally show a slow increase over time, which is not observed in any of the springs with shorter MTT's and springs at the northern region (see Fig. S6).

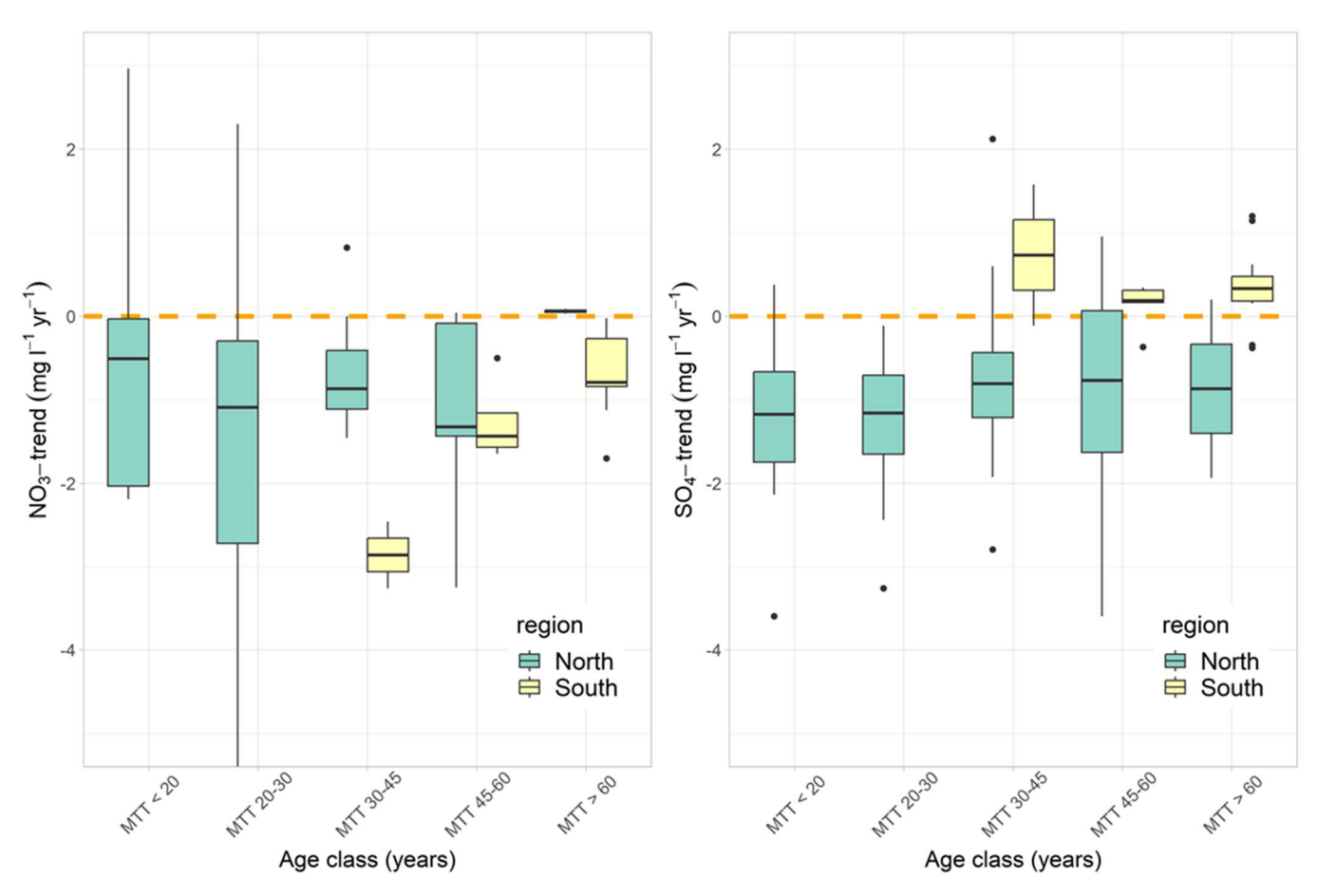


Fig. S6 Trend in the measured nitrate (left panel) and sulfate concentrations (right panel) over the period 2009 to 2018 for the northern springs (green) and southern springs (yellow). Decreasing trends in negative numbers and increasing trends in positive numbers. Decreasing trends for nitrate and sulfate occur in most northern springs, which is attributed to the decreasing loads of N and S in the agricultural leachate (e.g., Visser et al., 2009). In contrast, sulfate concentrations increase in the southern springs while nitrate concentrations decrease.

Together, this bears the suggestion that nitrate reduction coupled to pyrite oxidation is responsible for lower nitrate concentrations and elevated mobilized sulfate in those southern springs (e.g., Zhang et al., 2007). Therefore, we tested two alternative models in which denitrification coupled to pyrite oxidation removes nitrate from part of the outflowing groundwater. The first model assumed a 90% reduction after 50 years of travel time (run 10 in Table 1 of the main text). The second model was more stringent and assumed 50% nitrate reduction after 30 years and 90% after 50 years travel time (run 11). Only the stringent model was able to mimic the nitrate decline in the springs with MTT's > 60 year as is illustrated in Fig. 5F (main text). The conceptual model that we used assumes conservative transport through the unsaturated and saturated zone in the chalk for the first 30 or 50 years, and reactive flow after the transport is through the fractured sandstones of the underlying Vaals Formation. Effectively, this mimics the situation in which the older fraction that contributes to the spring is virtually nitrate-free, whereas the younger fraction is responsible for the nitrate discharge at the spring.

Fig. S7 illustrates the effect of the more stringent denitrification model on the nitrate evolution in 3 springs that drain the southern chalk plateaus. Obviously, applying this denitrification model for the southern chalk springs changes the forecasts for 2027 and 2035. The implication is that a larger number of southern springs is forecasted to be below the 50 mg/l EU water quality standard.

This is further illustrated in Fig. S8 which compares the denitrification models with the base case model for the young fraction, the MTT and the 2035 nitrate forecasts. The inclusion of a denitrification process shifts the MTT downward (up to 5 years, Fig. S8A and S8B) and the young fraction upward (up to a fraction of 0.05, Fig. S8C and S8D) for the southern springs. This resembles a larger contribution from young, nitrate containing water, and is explained by the fact that dilution with a large flow component of old water is no longer needed to simulate the relatively low nitrate concentrations at the springs. In other words: attenuation now substitutes dilution as the nitrate reducing mechanism. The effect on the nitrate 2035 forecast is pronounced, indicating that all the southern springs are predicted to comply with the 50 mg/l WFD standard by 2035 for the more stringent denitrification model (Fig. S8F). It is important to note that this result is not determined by conservative advective flow, but mainly the result of attenuating processes in the subsurface. This is not immediately clear when observing the spring water quality in the field (e.g., De Mars, 2023), as there are no indications for elevated iron concentrations because iron is probably precipitated as ironhydroxides during the mixing of the different water components at the spring outlets. Instead, the result is obtained by measuring the temporal changes of nitrate and sulfate, combined with modelling conservative transport which fails to explain the measured trends.

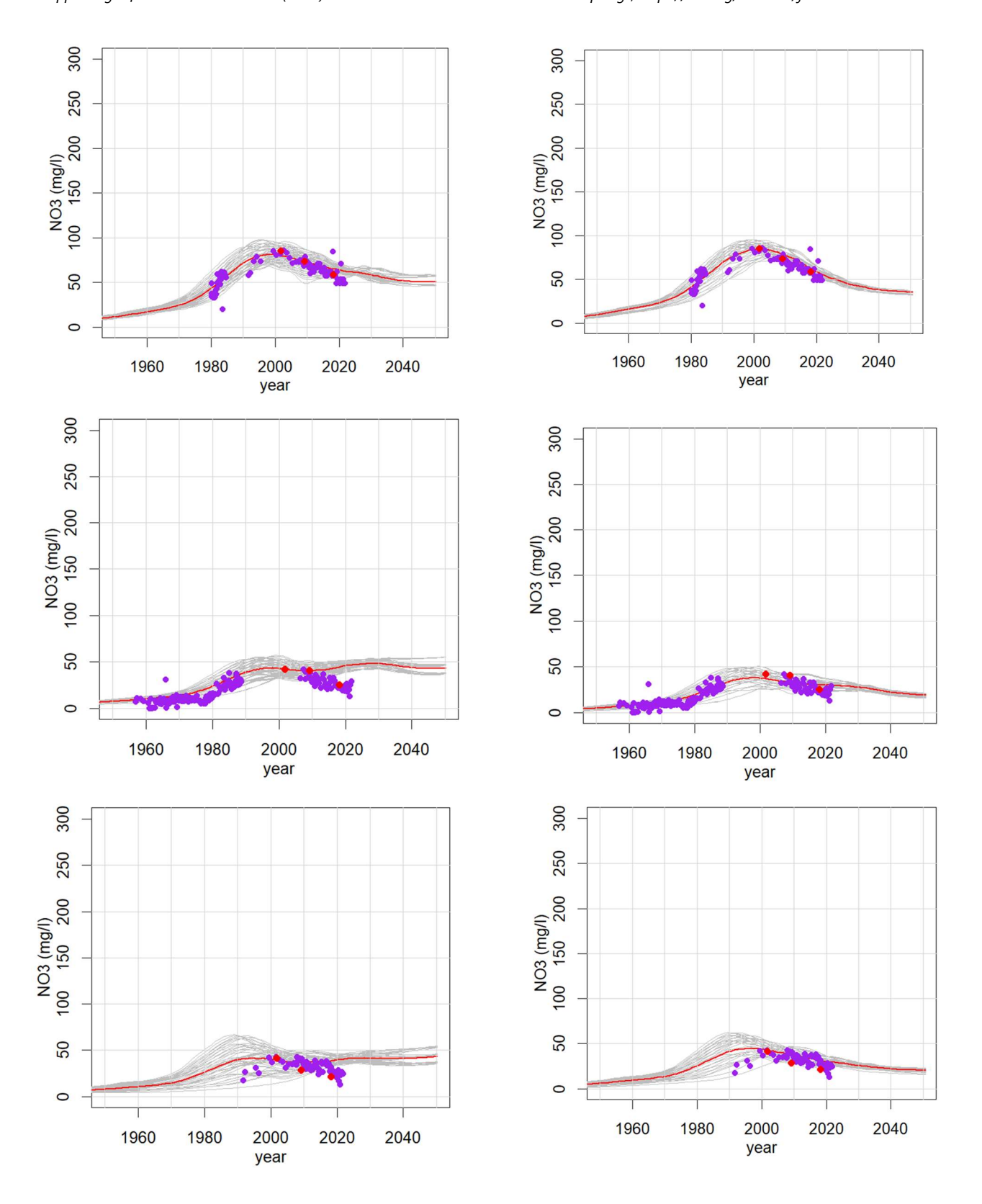


Fig. S7 Examples of nitrate reconstruction and forecasts for 3 southern springs (from top to bottom: z.001, z.028 and z.035). Comparison between base case model (left panels) and stringent denitrification model (right panels). Note the difference in model concentrations for the year 2050. Red symbols: RIVM low frequency time series, purple symbols: provincial high frequency series.

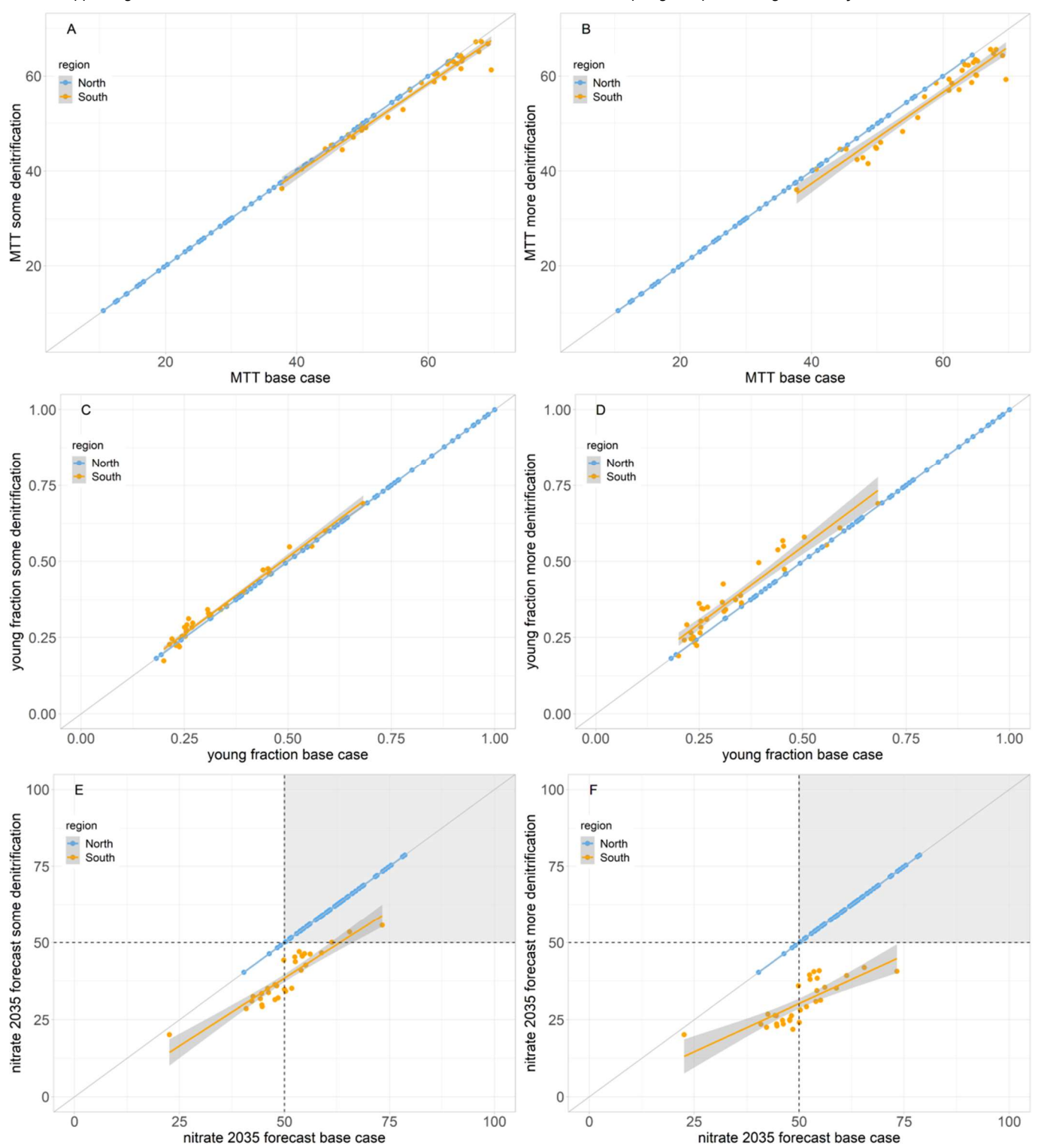


Fig. S8 Results of the comparison between the base case and the two denitrification cases. Left panels: some denitrification (A, C and E). Right panels: more stringent denitrification (B, D and F). Denitrification was only considered for the set of southern springs for which a flow contribution from the Vaals Formation is likely or possible. Alternative models are equal to base case models for the northern springs (shown for reference only). Lines and shaded areas represent a linear regression and its uncertainty.

S6 Hysteresis of the spring outlet concentrations relative to the nitrate leaching history

The nitrate concentrations at the spring outlets exhibit a clear hysteresis in relation to the nitrate concentrations that leach from the root zone of the farmlands (Figure S9). Spring nitrate concentrations are higher in the downward limb following the peak in N usage compared to concentrations prior to the peak. In the conservative model, this behavior is solely determined by the travel time distribution (TTD) of the springs, meaning by advective flow and mixing of flow contributions at the spring only, contrary to earlier work by Dessirier et al. (2023) which suggested a significant role of N storage in the soil compartment in their study catchments.

For springs n.002 (Fig. S9A) and z.001 (Fig. S9B), the outlet concentrations persist above 50 mg/l until around the year 2000, gradually declining toward the stabilized input concentration of 50 mg/l (represented by the black square) only after 2020. For spring z.039, which has a substantial contribution of water aged more than 80 years, the concentrations continue to rise long after the input load diminished, eventually stabilizing around (50,50) well beyond 2030. Considering denitrification processes, which are plausible for springs z.001 and z.039 which are partially supplied by water from the Vaals Formation, the concentrations decline earlier towards the stabilization point and below (Fig. S9B and S9D).

Overall, the hysteresis plots describe the loading of the groundwater system with nitrate, with initial slow increase of spring concentrations due to a contribution of nitrate-free, pre-1960 water and a delayed reaction after the input load began decreasing after 1985. Assuming conservative transport, the hysteresis patterns are entirely determined by the age distribution of the discharged water at the spring, while subsurface denitrification influences the shape in reactive cases. These findings corroborate earlier research by Sarrazin et al. (2023), whose sensitivity analysis demonstrated that the travel time in the subsurface and denitrification rate in the subsurface are important determinants for nitrogen legacies in receiving surface waters.

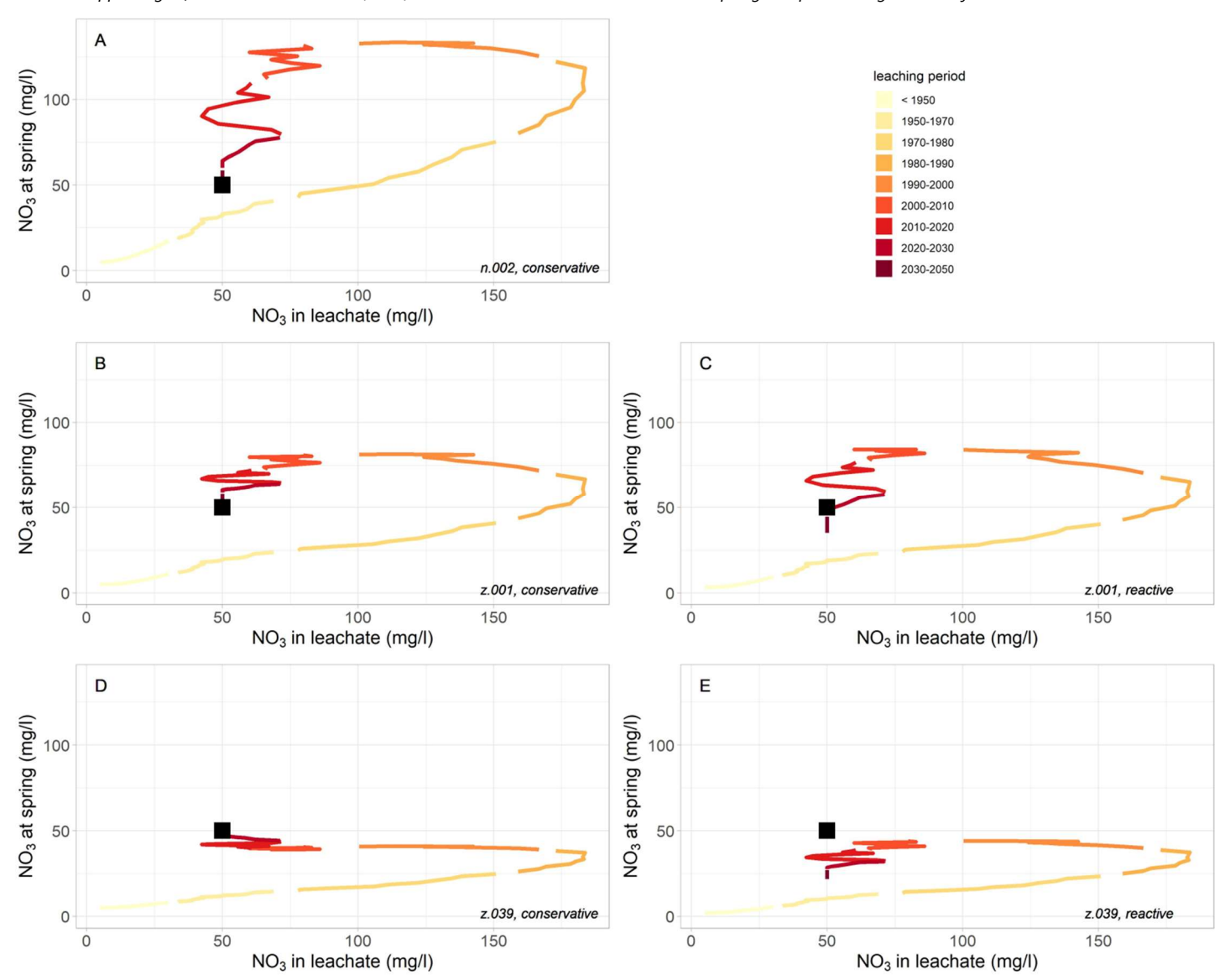


Fig. S9 Relation of the modelled nitrate concentration of three springs with the nitrate concentration leaching from the root zone over time. A: spring n.002, Elsloo, B+C: spring z.001 St. Brigida and D+E: spring z.039, Wijlre (see Figure S1 or Figure 1 for their locations). Graphs A, B and D represent the conservative base case model, graphs C and E the stringent denitrification case (see Section S6).